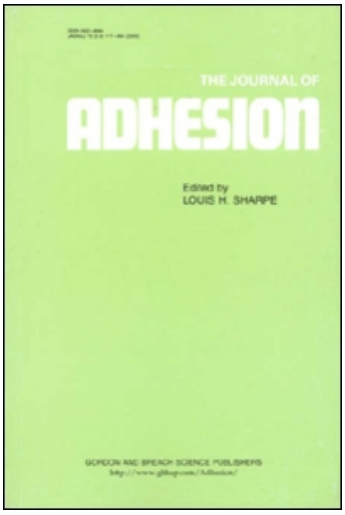

The Journal of Adhesion
Publication details, including instructions for authors and subscription information:
http://www.informaworld.com/smpp/title~content=t713453635

Influence of Aging on Autohesive Tack of Brominated Isobutylene-co-*p*-methylstyrene (BIMS) Rubber in the Presence of Phenolic Resin Tackifier

K. Dinesh Kumar[a]; Anil K. Bhowmick[a]; Andy H. Tsou[b]
[a] Rubber Technology Centre, Indian Institute of Technology, Kharagpur, India [b] Corporate Strategic Research, ExxonMobil Research and Engineering, Annandale, New Jersey, USA

To cite this Article Kumar, K. Dinesh , Bhowmick, Anil K. and Tsou, Andy H.(2008) 'Influence of Aging on Autohesive Tack of Brominated Isobutylene-co-*p*-methylstyrene (BIMS) Rubber in the Presence of Phenolic Resin Tackifier', The Journal of Adhesion, 84: 9, 764 — 787
To link to this Article: DOI: 10.1080/00218460802352942
URL: http://dx.doi.org/10.1080/00218460802352942

The Journal of Adhesion, 84:764–787, 2008

ISSN: 0021-8464 print/1545-5823 online
DOI: 10.1080/00218460802352942

Taylor & Francis
Taylor & Francis Group

Influence of Aging on Autohesive Tack of Brominated Isobutylene-co-*p*-methylstyrene (BIMS) Rubber in the Presence of Phenolic Resin Tackifier

K. Dinesh Kumar[1], Anil K. Bhowmick[1], and Andy H. Tsou[2]
[1]Rubber Technology Centre, Indian Institute of Technology, Kharagpur, India
[2]Corporate Strategic Research, ExxonMobil Research and Engineering, Annandale, New Jersey, USA

*The role of phenolic resin tackifier on autohesive tack of brominated isobutylene-co-*p*-methylstyrene (BIMS) rubber was studied by a 180° peel test with particular reference to aging. Phenolic resin showed very little effect on the unaged tack of BIMS rubber. The tack strength of the rubber/resin mixture marginally increased at 1 phr resin concentration, beyond which it decreased. Based on the data on the compression creep, maximum tensile stress, and viscoelastic properties of the rubber/resin mixtures, phenolic resin did not enhance the interfacial viscous flow behavior of the rubber/resin mixtures. The results from dynamic mechanical analysis (DMA) and scanning electron microscopy (SEM) confirmed the existence of a phase-separated morphology in the rubber/resin blends even at low resin concentration. Upon aging at 100°C for 36 h, the rubber/resin blend containing 1 phr of phenolic resin showed further increase in tack strength which was attributed to migration of the tackifier to the rubber surface and the changes in the compression creep, viscoelastic behavior, and maximum tensile stress of the rubber/resin mixtures. This is also a function of aging time. Surface energy analysis by contact angle measurement, Fourier Transform Infrared Spectroscopy (FT-IR/ATR) studies, and surface roughness measurement by atomic force microscopy (AFM) elucidate the enrichment of the phenolic resin on the rubber surface upon aging and the mechanism of enhanced tack strength.*

Keywords: 180° peel; Aging; BIMS; Compatibility; Phenolic resin tackifier; Tack

Received 17 December 2007; in final form 3 July 2008.
Address correspondence to Anil K. Bhowmick, Rubber Technology Centre, Indian Institute of Technology, Kharagpur 721302, India. E-mail: anilkb@rtc.iitkgp.ernet.in

1. INTRODUCTION

The terms autohesion, self-adhesion, and self-tack refer to attraction between identical bodies. In the tire industry the autohesion of raw or compounded rubbers has been considered to be one of the most important properties when building rubber articles from uncured rubber stocks. If a rubber stock has too little tack, it is difficult to build rubber articles, because the rubber layers tend to fall apart before cure. This results in decreased productivity and increased scrap. Consequently, the right amount of tack is highly desirable to produce rubber articles of good and uniform quality at a constant rate.

It is generally believed that the tack is determined by three fundamental processes [1–3]. First, the polymer chains from each surface must come in to intimate molecular contact. This requires viscous flow of material near the interface and displacement of surface impurities. Next, chains interdiffuse across the interface and become entangled with one another. Finally, the material must have a high cohesive strength so that the bond is able to resist separation. It has been reported earlier that diffusion of polymer chains across the interface is the major factor for bond formation [3–5].

However, it has also been reported that an intimate molecular contact precedes the interdiffusion of polymer chains [6–9]. Accordingly, the bond formation kinetics is influenced by both contact flow and interdiffusion of polymer chains [2]. Therefore, enhancing the molecular contact will produce a high number of polymer chain segments that can diffuse across the interface resulting in a better bond formation.

In the literature, the tack behavior of various elastomers has been reported. Bhowmick and Gent [10] have examined the effect of interfacial bonding on the self-adhesion of SBR and chloroprene (CR) elastomers. The tack and green strength of the unfilled and filled blends of bromobutyl and EPDM rubbers have been reported [11,12]. The tack and diffusion properties of silicone and EPDM rubbers are also available [13]. van Gunst *et al.* [14] have studied the inherent tack of EPDM rubber compounds.

In the rubber industry, tackifiers are used to improve the tack and tack retention of compounded elastomers [2,3]. Tackifiers are generally added at lower concentration to improve autohesion. Three major types of tackifiers are: hydrocarbon tackifiers, rosin acids and its derivatives, and phenol-formaldehyde resins [15–17]. Tackifying resins typically have a molecular weight of *ca.* 2000 or less. Literature related to the use of tackifying resins at higher resin concentrations for pressure sensitive adhesive application are available [17–19].

The use of tackifiers at relatively lower concentrations for improving autohesion and green strength of various elastomers has also been reviewed [2,3], although the fundamental understanding of tack between elastomer compounds with low amounts of tackifiers is still insufficient.

Brominated isobutylene-co-*p*-methylstyrene (BIMS) rubber is a fairly new commercial rubber for a number of industrial applications both in tire and non-tire areas. In tire sectors, this is used as a major component in tire tubes, sidewalls, and inner liner and its tack properties are important for the success of their applications. Kumar *et al.* [20] have investigated the tack and green strength of BIMS rubber and its blends with reference to level of bromination, fillers, and blend ratio.

Presently, there is no report on the effect of tackifier on the tack behavior of BIMS rubber. In this paper, the role of a non-heat-reactive phenolic tackifier on tack strength of BIMS rubber has been investigated with special reference to: (a) tackifier concentration (1, 3, 5, 7, 10, and 30 phr); (b) rubber-resin compatibility; (c) viscoelastic properties of rubber-resin blends; (d) morphology; and (e) aging conditions.

In the literature, an increase in the autohesion of general purpose elastomer compounds has been observed at tackifier concentrations as low as 1–2% using a phenolic resin [2]. However, the mechanism by which the phenolic resin increases the autohesion of the elastomers is not properly understood [15]. Moreover, no conclusive evidence has been presented elsewhere to support the earlier proposed mechanisms. The purpose of this paper is also to investigate the mechanism of action of a phenolic resin in this new rubber under different conditions. (*i.e.*, before aging and after aging).

2. MATERIALS AND METHODS

2.1. Materials

Brominated isobutylene-co-*p*-methylstyrene, or BIMS (grade: Exxpro^{TM} 3035; benzylic bromine of 0.47 ± 0.05 mole % and 2.0 mole % of p-methylstyrene, Mooney viscosity of 45 ± 5 at ML1 + 8 125°C and $M_w = 450{,}000$) was supplied by the Exxon Mobil Chemical Company (Baytown, TX, USA) and Octylphenol-formaldehyde thermoplastic phenolic resin tackifier (grade: SP1068; softening point of 85–95°C and glass transition temperature of 35°C) was supplied by Schenectady International Inc. (New York, USA).

2.2. Preparation of Filled Samples

Preparation of Rubber-Resin Blend

The mixes were prepared in a Brabender Plasticoder (model PLE-330, capacity 65 ml, Duisberg, Germany) at 110°C and 60 rpm. BIMS was placed in the Brabender and sheared for 2 min and then the tackifier was added and mixing was continued for an additional 3 min. The neat BIMS rubber was also processed for 4 min under the same condition. The composition of the mixes prepared is reported in Table 1.

2.3. Preparation of the Test Samples

For determination of tack strength, rubber sheets (10 cm wide × 15 cm length × 2.5 mm thick) were prepared by pressing them at 100°C for 5 min between smooth Mylar® sheets at 5 MPa pressure in an electrically-heated press (David Bridge, Castleton, England). One side of the rubber sheet was backed by a fabric having ~1 mm thickness. The samples were then left for 20 ± 2 h before testing, for conditioning the samples. For the determination of maximum tensile stress, the rubber sheets (10 cm wide × 15 cm length × 2.5 mm thick) were prepared by pressing them at 100°C for 5 min between sheets of smooth aluminum foil at 5 MPa pressure in an electrically-heated press.

2.4. Measurement of Tack Strength

In this study, tack strength was measured by a 180° peel test. The strips (2.54 cm wide × 7.5 cm, length × 2.5 mm thick) were cut from the previously prepared sheet. For unaged samples, Mylar sheet was peeled just prior to testing. Selected samples were allowed to age in an aging oven at 100°C for 36 h. Tack testing was performed by placing the two samples together with a Mylar insert at one end

TABLE 1 Composition of Mixes Prepared

Sample number	Designation	BIMS rubber (grams)	Phenolic resin (phr)*
1	B	100	0
2	BSP1	100	1
3	BSP3	100	3
4	BSP5	100	5
5	BSP7	100	7
6	BSP10	100	10
7	BSP30	100	30

*phr-parts per hundred grams of rubber.

(contact area 2.54×5.5 cm). A load of 2 kg was applied in each case ($\sim$14.0 kN/m^2) by means of a specially designed hand press, having a provision for applying variable loads. In all cases, the contact time was 15 seconds. After sufficient contact time was reached, the average force required to separate the two strips was measured by using a computerized Zwick/Roell Z010 (Zwick/Roell, Ulm, Germany) Universal Testing Machine at 25°C. The rate of peeling was 250 mm/min. The data were analyzed using testXpert II software of the Zwick/Roell Universal Testing Machine. The tack strength, G_a (N/m), was calculated using the formula [10]:

$$G_a = 2F/w, \tag{1}$$

where F is the average force (N) required for peeling and w is the width (m) of the sample. For each system, four samples were tested and the results were averaged. For all samples, the peel force, F, was taken to be the average value where there was nearly constant peel force with small and random fluctuations.

2.5. Measurement of Maximum Tensile Stress from Stress-Strain Curves

Green strength was measured by determining the maximum tensile stress from the stress-strain curves. Maximum tensile stress measurement was done according to ASTM D412–98T. Dumbbell-shaped specimens were punched from the prepared sheets and maximum tensile stress was measured in a computerized Zwick/Roell Z010 Universal Testing Machine at 25°C at a separation rate of 50 mm/min. The data were analyzed by the testXpert II software of the Zwick/Roell Universal Testing Machine. The maximum tensile stress was taken as the maximum stress in the stress–strain, σ-ε, curve. The tensile stress is defined as the ratio of the applied force to the initial, undeformed cross sectional area, and the tensile strain is based on the initial sample length. From the tensile stress-strain, σ-ε, curves, some of the important features such as, the maximum stress, σ_{max}, the strain at break, ε_b, and the work done per unit volume, W_b (area under the stress-strain, σ-ε curve), were identified. Four samples were tested for each system and averages of the results were reported.

2.6. Compression Creep Measurement

The contact flow was determined by compression creep measurements. Compression creep was measured using a special device which consists

of a cylinder of 4 mm diameter attached to a dial gauge (0.01 mm accuracy). A sample of 4 mm diameter was cut from the stock sheet. The sample was then placed in this device under load ($\sim$14.0 kN/m^2) and the change in thickness was measured as a function of time. The sample thickness and the load applied were the same as those in tack measurements. The compression creep was calculated as the change in thickness (δl) divided by the initial thickness (l). For each system, three samples were tested and average results were reported.

2.7. Dynamic Mechanical Analysis (DMA)

2.7.1. Temperature Sweep Test

Temperature sweep test was carried out in a dynamic mechanical analyzer (DMA-2980 from TA Instruments, New Castle, DE, USA), in tension mode geometry in the temperature range of -100°C to 100°C for neat BIMS and BIMS-resin blends using a constant frequency of 1 Hz and a constant strain of 0.1%. The sample dimension was 6.25 mm wide $\times$ 30 mm length $\times$ 2.5 mm thick.

2.8. Fourier Transform Infrared Spectroscopy (FT-IR)

The infrared spectra of the samples were recorded with a Perkin-Elmer FT-IR spectrophotometer (Shelton, CT, USA). FT-IR/ATR spectra of the films of thickness 0.3 mm were taken at room temperature (25°C) for surface composition analyses of the unaged and the aged films. In order to obtain base spectra of the resin, FTIR transmission spectra were obtained from resin/KBr pellets, which were mixes of KBr powder and resin. All powder and film samples were scanned from 4000 to 400 cm^{-1} with a resolution of 4 cm^{-1}. All spectra were reported after an average of 32 scans.

2.9. Surface Energy Measurements

The values of the dispersive, γ_s^D, and polar, γ_s^P, components of surface energy for the aged and the unaged samples were obtained using a contact angle meter (Kernco, Model G-II from Kernco Instruments, EI Paso, TX, USA). The sessile drop method, employing 2 µl drops of different probe liquids, was applied for contact angle measurements. The liquids used for the contact angle measurements were triply distilled water and special grades of ethylene glycol, formamide, and methylene diiodide obtained from Lancaster Synthesis (Morecambe, England). Each contact angle quoted is the mean of at least five measurements with a maximum error in θ of $\pm 1^\circ$. All investigations

were carried out in vapor saturated air at $20 \pm 2^{\circ}C$ in a closed sample box. The advancing contact angle value of probe liquids at 1 min was observed in all cases.

2.10. Surface Morphology Study

2.10.1. Scanning Electron Microscope (SEM) Studies

The dispersion of phenolic resin in the rubber matrix was examined by a JEOL, JSM 5800 (Japan) scanning electron microscope (SEM) after sputter coating the samples with gold.

2.10.2. Atomic Force Microscope (AFM) Imaging

The morphology of rubber-resin blends, before and after aging, was analyzed by measuring the roughness values (R_a and R_q) of the sample surface using atomic force microscopy (AFM). AFM studies were carried out in air at ambient conditions ($25^{\circ}C$, 60% RH) using a multimode AFM (Veeco Digital Instruments, Santa Barbara, CA, USA). Topographic height and phase images were recorded in the tapping mode atomic force microscope (TMAFM) with the set point ratio of 0.9, using a long tapping mode etched silicon probe (LTESP) tip having a spring constant of 48 N/m. For each sample, a minimum of three images were analyzed. The cantilever was oscillated at a resonance frequency (ω_0) of $\sim$280 kHz.

The root-mean-square roughness, R_{RMS}, is defined as the standard deviation of feature height, Z, within a given image area and it is given by the equation below:

$$R_{RMS} = \sqrt{\sum (Z_i - Z_{av})^2 / n}. \quad (2)$$

The mean surface level is defined as the line about which roughness is measured. Z_{av} is the average Z value and Z_i is the current Z value and n is the number of points within the given area. Roughness has been calculated from the AFM images of the unaged and the aged samples of same scan size.

3. RESULTS AND DISCUSSION

3.1. Effect of Tackifier Concentration on Tack Strength of BIMS Rubber

The tack strength, G_a, of BIMS/phenolic resin blends is shown in Figure 1. For these rubber/tackifier mixtures, the addition of tackifier did not show significant improvement in the tack strength. The tack

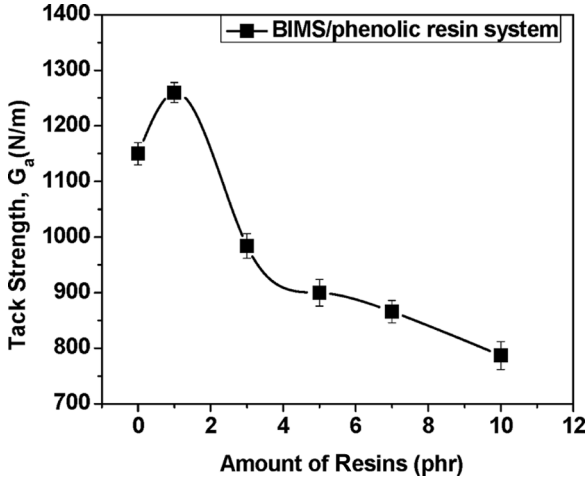

FIGURE 1 Effect of loading of resin on tack strength of BIMS-phenolic resin system.

strength of BIMS rubber increased at 1 phr loading of phenolic resin. With the continued increase in loading of resin beyond 1 phr, there was a drop in tack strength to below the tack strength of neat BIMS rubber. The force *vs.* distance curve of the 180° peel test is shown in Figure 2 where variations of peel force with distance are relatively small.

Generally, most rubber/tackifier mixtures have lower viscosity in comparison with the neat rubber which, in turn, can facilitate the compression creep and diffusion of polymer chains at the interface without any significant compromise in maximum tensile stress [3]. However, here BIMS/phenolic resin mixtures did not show this type of behavior. In Figure 3, the compression creep curves of neat BIMS rubber and resin loaded samples are shown. Only slight increases in compression creep can be seen in resin loaded samples. This suggests that the addition of resin did not decrease the elastomer viscosity to facilitate the compression creep. Moreover, the maximum tensile stress of BIMS rubber gradually decreased up to 5 phr resin concentration, beyond which the maximum tensile stress increased with resin loading (Figure 4). In general, in an uncured compound, the incompatible resin will exist in a phase-separated state and the hard resin will function as reinforcement up to the softening point of the resin [21]. The limited compatibility between phenolic resin and BIMS rubber, to be discussed in later sections, led to incompatible resin dispersions in BIMS rubber. σ_{max} and W_b values of the sample BSP10 are 0.25 MPa and 0.17 Nm, whereas the σ_{max} and W_b values of neat BIMS rubber

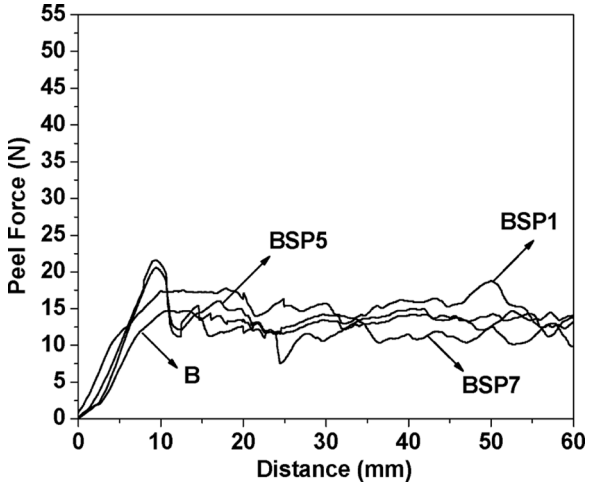

FIGURE 2 Peel force-distance curves for BIMS-phenolic resin system. See Table 1 for designations B, BSP1, etc.

are 0.26 MPa and 0.20 Nm, respectively. The addition of 10 phr of phenolic resin did not cause any significant reduction in the maximum tensile stress of the BIMS rubber. Moreover, the W_b value of sample BSP10 decreased considerably due to the reduction in ε_b value. The reduction of the W_b value will lower the potential of the rubber/resin

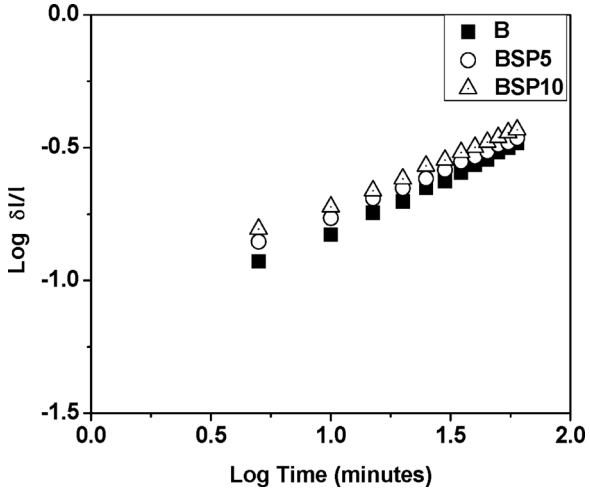

FIGURE 3 Compression creep ($\delta l/l$) of B, BSP5, and BSP10.

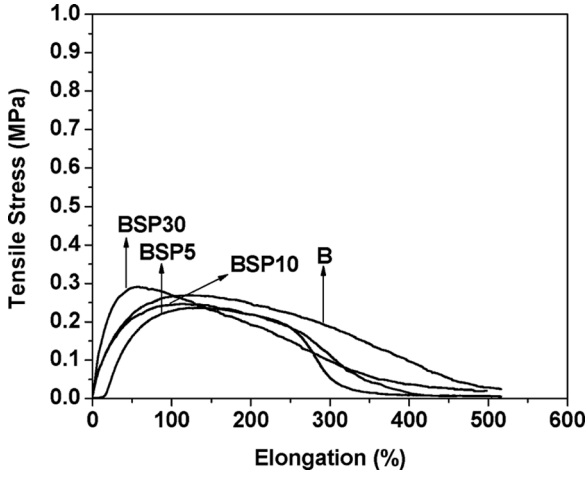

FIGURE 4 Tensile stress *vs*. elongation plots of B, BSP5, BSP10, and BSP30.

mixture to dissipate a greater amount of energy during the bond separation process. Moreover, the gradual increase of the σ_{max} values at higher resin loading (>5 phr) will decrease the contact area between the interfaces. For all these reasons, the tack strength of the rubber/resin mixtures has significantly decreased with increase in resin loading.

3.2. Dynamic Mechanical Properties of BIMS-Phenolic Resin System

Figures 5a–b shows the tan δ and Log E′ plots against temperature for three representative samples. (The results of other samples are omitted for clarity in the figure.) For BSP10 and BSP30, there is no significant change in the tanδ peak temperature and a high temperature tan δ peak is apparent at approximately 75°C. Also, at resin concentration of 30 phr, a second transition can be seen in the storage modulus curve at about 75°C, confirming the phase separation of phenolic resin tackifier in the BIMS rubber. Commonly, a tackifier which has good compatibility with rubber will cause an increase in T_g, broadening of the transition region, and a decrease in the plateau modulus [22]. Here, the rubber/tackifier mixtures did not show the expected shift of the tan δ peak temperature and also there was no depression of the storage modulus in the plateau zone. In the rubbery plateau region, the storage modulus is determined primarily by the density

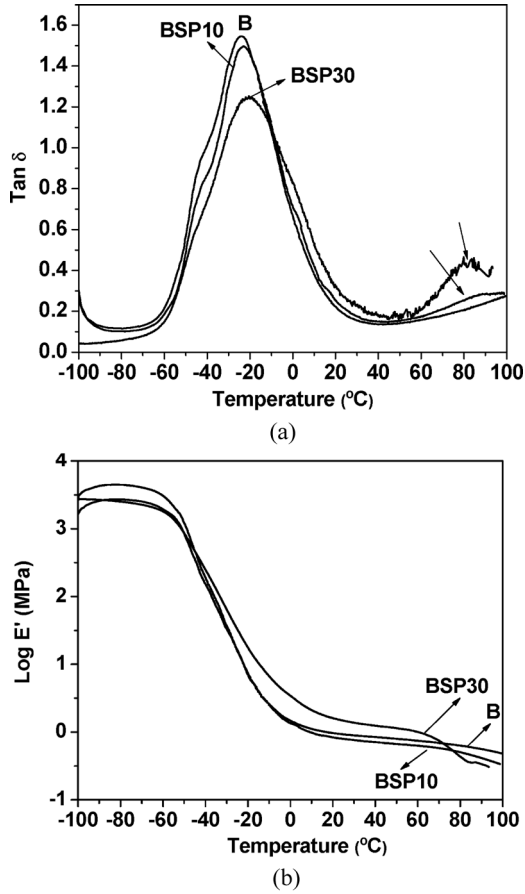

FIGURE 5 (a) Tan δ *vs*. temperature curves of B, BSP10, and BSP30; (b) Storage modulus (Log E′) *vs*. temperature curves of B, BSP10, and BSP30.

of the entanglements. In this region, the tackifier acts as a diluent and causes a decrease in the storage modulus values (by the reduction of the entanglement density) which, in turn, will facilitate the diffusion of the rubber molecules at the autohesive joints. However, here, the phenol formaldehyde resin tackifier did not show any significant dilution effect in the rubbery plateau region of the base polymer. These results suggest the limited compatibility between the phenolic resin and the BIMS rubber and also elucidate the limited viscous flow behavior of rubber/resin mixtures at contact. Burhans and Soldators [23] reported that compatibility of SBR, butyl, and polybutadiene

rubbers with phenolic resin has a great influence on the autohesive tack of the rubber/resin mixtures. The entanglement density in the rubbery plateau zone can be accurately estimated from the parameters such as entanglement molecular weight (M_e) and network density (υ) (moles of network strands per cubic centimeter). The aforementioned parameters were calculated to understand the diluent effect of phenol formaldehyde resin tackifier in the rubbery plateau modulus. The entanglement spacing molecular weight (M_e) can be estimated from the plateau modulus (G_n^0) as follows [24–27]:

$$M_e = \frac{\rho RT}{G_n^0}, \tag{3}$$

where ρ is the density of the polymer or blend, R is $8.31451\,J/K \cdot mol$, T is the absolute temperature where G_n^0 is located, and G_n^0 is determined from the storage modulus (G′) at the onset of the rubbery region (usually where tan δ reaches a minimum following the prominent maximum).

Furthermore, the plateau modulus could be related to the network density (υ) (the moles of network strands per cubic centimeter) [26,27]. The relationship between the plateau modulus and network density (υ), is given by the equation:

$$G_n^0 = \upsilon RT. \tag{4}$$

On rearranging the above equation, the network density can be calculated from the following equation:

$$\upsilon = \frac{G_n^0}{RT} \tag{5}.$$

The G_n^0, M_e, and (υ) values of the neat BIMS rubber and BIMS/phenolic resin blends are reported in Table 2. The plateau modulus

TABLE 2 Effect of Phenolic Resin Tackifier on the Viscoelastic Properties of the BIMS Rubber

Sample number	Designation	Plateau modulus G_n^0 (MPa)	Entanglement molecular weight (M_e) (g/mol)	Network density $\nu \times 10^{-4}$ (mol/cm^3)
1	B	0.79	3345	2.9
2	BSP1	0.67	3569	2.7
3	BSP10	0.70	3400	3
4	BSP30	1.20	2219	4.5

(G_n^0) of neat BIMS rubber decreased marginally below 10 phr loading of the phenol formaldehyde resin tackifier. However, at higher loading of the phenolic resin tackifier (>10 phr), there was an abrupt increase in the plateau modulus values, which can be attributed to the mild reinforcing character of the phase separated phenolic resin tackifier. This also resulted in the reduction of the entanglement spacing molecular weight (M_e) with the simultaneous increase in the network density (υ) values. This confirms the very limited diluent effect of the phenol formaldehyde resin tackifier in the rubbery plateau zone. It should be pointed out that the lack of dilution effect of the phenol formaldehyde resin tackifier in the rubber plateau region of the BIMS rubber will decrease the interfacial contact compliance and could reduce the contact areas which could lead to poor autohesion.

3.3. Morphological Analysis of BIMS-Phenolic Resin Mixture

The SEM photomicrographs of the samples BSP1 and BSP3 are shown in Figures 6a–b. White resin particles are observed on the surface of the rubber. Figure 6b shows bulk phase separation of the phenolic resin in the BIMS rubber matrix. This suggests the existence of a two-phase morphology even at 3 phr resin loading. This observation is in line with DMA analysis of the rubber/resin mixtures regarding the compatibility between the blend components. Resin particles are dispersed randomly in BSP3 with the particle size mostly greater than 20 μm. This phase separation of resin in the rubber matrix is attributed to the limited compatibility between BIMS rubber and phenolic resin. It is well known that [15,28–31] the tackifier/rubber blends, which are compatible in bulk, also undergo tackifier controlled migration to the surface, thereby facilitating the self-bond formation by reducing the entanglement of molecules in the surface. However, here, totally phase-separated resin particles are seen on the rubber surface—thereby creating a stiff brittle layer of resin on the surface which will reduce the true area of contact at the interface. For this reason, it can prevent the diffusion of polymer molecules between the joints and will lead to poor tack strength. Figure 6a shows relatively uniform dispersion of resin particles with particle size mostly ranging well below 10 μm at BSP1 surface. At this low resin concentration, the relatively finer dispersion of the resin particles in BSP1 may not affect the interfacial self diffusion of the BIMS and, at the same time, may lower the BIMS surface entanglement, which could further facilitate the self-diffusion. It may be for these reasons that the tack strength of the rubber/resin mixture containing 1 phr resin concentration was raised slightly from BIMS rubber.

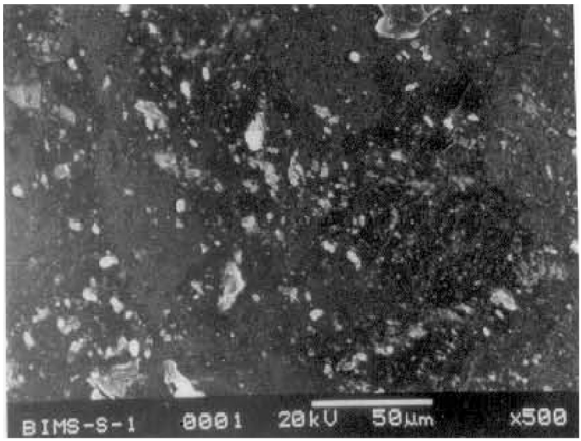

(a)

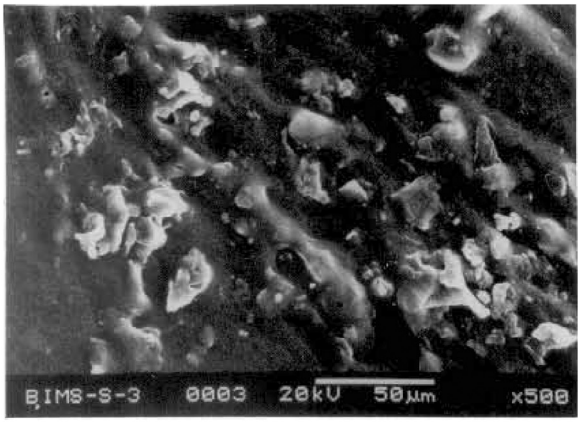

(b)

FIGURE 6 (a) SEM photograph of sample BSP1. (b) SEM photograph of sample BSP3.

3.4. Effect of Aging on Tack Strength of Pristine BIMS and Rubber-Resin Blend

The samples B and BSP1 were aged at 100°C for 36 h and at 40°C for 72 h. Interestingly, significant changes were observed only at 100°C. Therefore, the following paragraphs discuss the tack behavior of samples B and BSP1 which were aged at 100°C for 36 h. After aging at 100°C, the sample B showed diminished (17% reduction) tack strength (Figure 7). After aging, the creep of sample B (pristine BIMS) marginally increases when compared with its unaged counterpart (Figure 8).

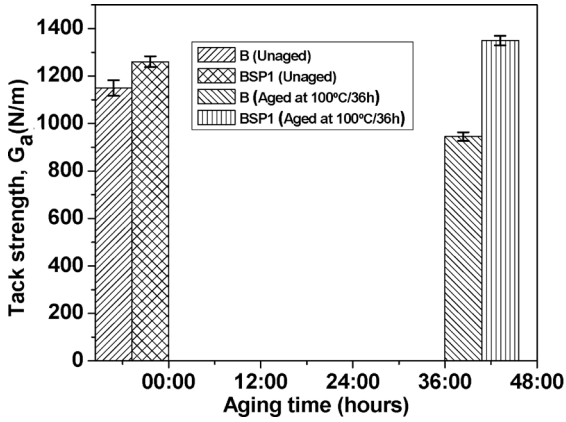

FIGURE 7 Effect of aging on tack strength of B and BSP1 (aged at 100°C for 36 h).

The increase in compression creep of the sample B (after aging) is attributed to the softening of the rubber matrix due to aging. During high-temperature aging at 100°C, some degradation of BIMS rubber (radical-initiated depolymerization of isobutylene) occurred which could lead to a softer and weaker rubber. This argument is supported by the shifting of the tan δ peak temperature of the sample B (aged) to lower temperature (Figure 9). Furthermore, the depression of E′ of the

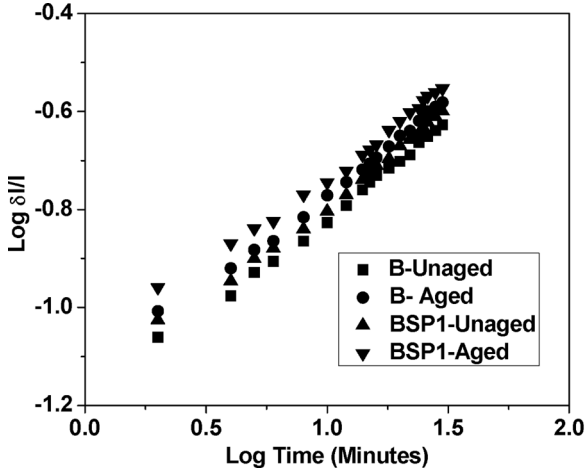

FIGURE 8 Compression creep ($\delta l/l$) of B and BSP1 (aged at 100°C for 36 h).

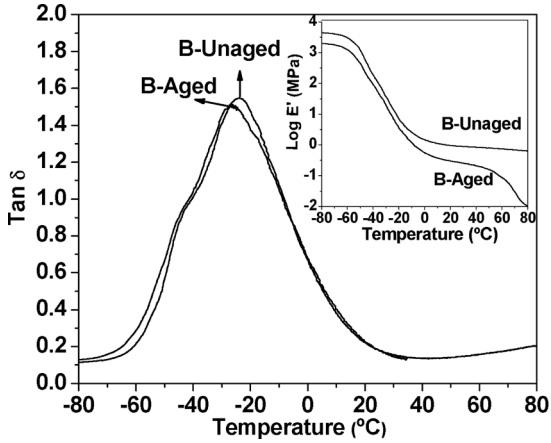

FIGURE 9 Tan δ *vs*. temperature curves of B (aged at 100°C for 36 h). (Inset) Log E′ *vs*. temperature curves of B (aged at 100°C for 36 h).

sample B (aged) in the plateau and terminal zone also provides evidence for some degradation of BIMS rubber upon aging (given as inset of Figure 9). Although the compression creep increases, there is a significant drop in maximum tensile stress after aging (Figure 10). Also, the elongation at break is reduced (given as inset of Figure 10). Therefore, an increase in compression creep can hasten the bond formation,

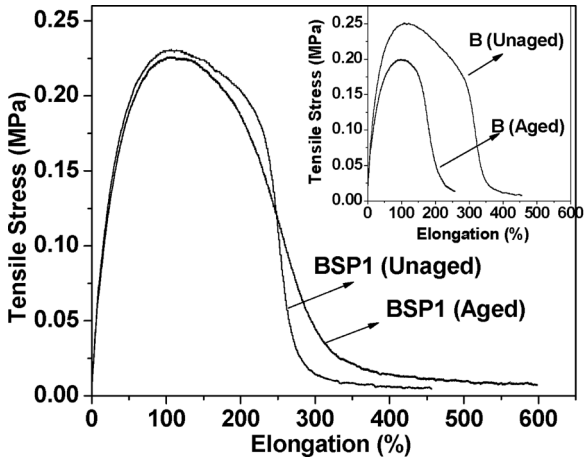

FIGURE 10 Tensile stress *vs*. elongation of BSP1 (aged at 100°C for 36 h). (Inset) Tensile stress *vs*. elongation of sample B (aged at 100°C for 36 h).

but a significant drop in maximum tensile stress will result in poor bond breaking resistance.

On the other hand, upon aging, the tack strength of the sample BSP1 increased. The tack strength of aged sample BSP1 was nearly 20% higher than the tack strength of the unaged neat BIMS rubber. The following paragraphs discuss the probable reasons for the enhancement of the tack strength of the sample BSP1 upon aging. The compression creep of sample BSP1 (after aging) is significantly higher than its unaged counterpart (Figure 8). There is a 20% increase in $\delta l/l$ at 10 minutes compression. Although there is no negative shift of the tan δ peak temperature, the storage modulus (E′) is reduced in the plateau zone (Figure 11) with aging. At 25°C, the values of E′ of the unaged and the aged samples are 0.74 MPa and 0.38 MPa, respectively. Furthermore, there is no reduction in the maximum tensile stress of the sample BSP1 after aging and the elongation at break actually was raised (Figure 10). Hence, there appears to be a good balance between the compression creep and the maximum tensile stress of the rubber/resin mixture after aging in order to increase the tack strength.

At this juncture, it is interesting to note that the tackifiers are found to be more enriched on the rubber surface after aging the sample BSP1. Here, there is clear evidence to prove the migration of the phenolic resin tackifier to the rubber surface upon aging. Figures 12a–b show the AFM pictures of the unaged and the aged

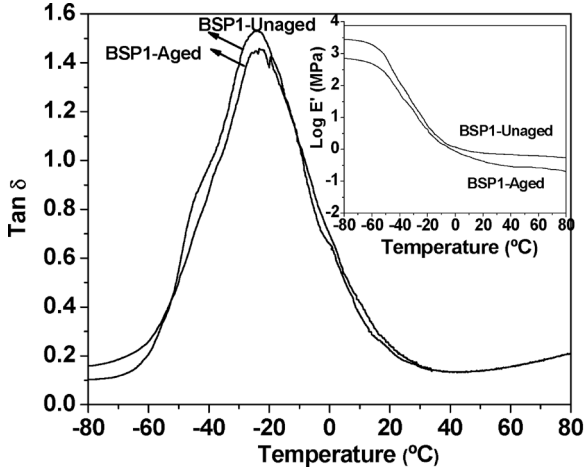

FIGURE 11 Tan δ *vs.* temperature curves of BSP1 (aged at 100°C for 36 h). (Inset) Log E′ *vs.* temperature curves of BSP1 (aged at 100°C for 36 h).

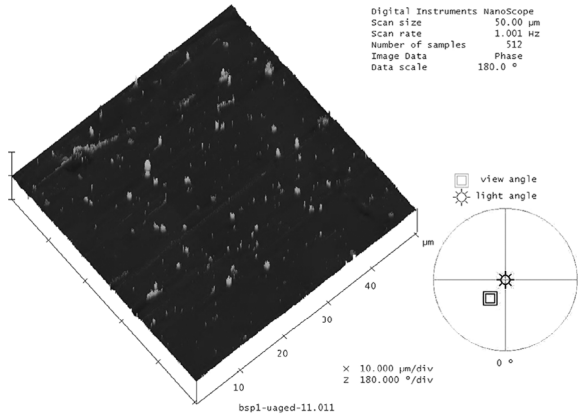

(a)

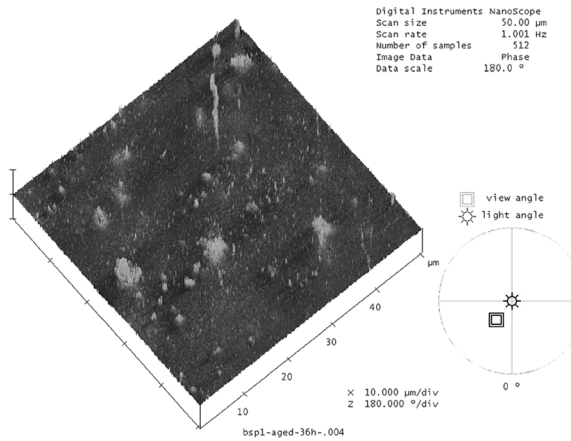

(b)

FIGURE 12 (a) Regular three-dimensional morphology of the phase image for sample BSP1 (unaged). (b) Regular three-dimensional morphology of the phase image for sample BSP1 (aged at 100°C for 36 h).

surfaces of the sample BSP1. Comparison of the two figures showed higher resin concentration on the rubber surface after aging. White resin particles were found to be enriched on the rubber surface after aging (Figure 12b). Roughness analysis from these AFM pictures revealed increases in *Z*-range and RMS value of the aged sample when compared with those of the unaged one. This suggests migration of the

TABLE 3 Roughness of Sample B and BSP1 (Unaged and aged)

Sample number	Designation	Image.Z range	Image.Rms (R_q)	Image.R_a
1	B (Unaged)	1.68	0.09	0.06
2	BSP1 (Unaged)	123.48	5.76	3.12
3	BSP1 (Aged at 100°C for 36 h)	124.92	6.01	4.11

phenolic resin to the BIMS rubber surface upon aging. The Image. Z range, Image.Rms (Rq), and Image.Ra values of the samples B and BSP1 (unaged and aged) are presented in Table 3.

Although migration of the tackifier to the rubber surface is suggested from the small increase in the surface roughness values of the aged sample BSP1, the surface region is not brittle and it is still rubbery (no change in T_g of BSP1, compared with that of B upon aging). As long as the surface layer remains rubbery, the bond formation will be hastened by the increased chain dilution of the rubbery molecules in the presence the tackifier at the surface. Moreover, the polar phenolic resin in the surface will increase the compression creep and diffusion of molecules at the interface due to the existence of the strong polar interfacial attraction between joining surfaces. It may be for this reason that the tack strength increased.

The contact angle of different probe liquids on the sample BSP1 (unaged and aged) further substantiates the enrichment of phenolic resin tackifier on the BIMS rubber surface after aging. The contact angle of liquids on samples were analyzed in accordance with the following theory in order to obtain values of the polar and dispersive components of the surface free energies of the samples B and BSP1 (aged and unaged). The van der Waals' forces of interaction between the liquid droplet and the solid are the sum of the polar and the dispersion forces. The Young equation gives the following relationship for the contact angle, θ [32,33]:

$$\gamma_S = \gamma_{SL} + \gamma_{LV} \cos\theta. \tag{6}$$

In the above equation, γ_S is the surface tension of the solid, γ_{LV} is that of the liquid in equilibrium with its saturated vapour, and γ_{SL} is the interfacial tension between the solid and the liquid. The surface tensions of both solid and liquid are the sum of dispersive components (distinguished by superscript D) and polar components (distinguished by superscript P), *i.e.,*

$$\gamma_S = \gamma_S^D + \gamma_S^P \tag{7}$$

$$\gamma_L = \gamma_L^D + \gamma_L^P. \tag{8}$$

The variables are related by Equation (9), which assumes that the attractive forces between molecules across the interface are the geometric mean of the forces between pairs of like molecules [34].

$$\frac{\gamma_L(1+\cos\theta)}{2(\gamma_L^D)^{1/2}} = (\gamma_S^P)^{1/2}\frac{(\gamma_L^P)^{1/2}}{(\gamma_L^D)^{1/2}} + (\gamma_S^D)^{1/2} \tag{9}$$

If the left-hand side of the equation (9) is plotted against $(\gamma_L^P)^{1/2}/(\gamma_L^D)^{1/2}$, the graph should be linear with intercept $(\gamma_S^D)^{1/2}$ and slope $(\gamma_S^P)^{1/2}$. A plot of this type for sample B is shown in Figure 13. Values of the dispersive and polar components of surface energy for sample B obtained from it by linear regression analysis are $\gamma_S^D = 14 \pm 2\,\mathrm{mN/m}$ and $\gamma_S^P = 25 \pm 2\,\mathrm{mNm^{-1}}$. Similarly, the values of the dispersive and polar components of surface energy for the sample BSP1 (unaged and aged) were identified and the results are plotted in Figure 14. The values of surface parameters for the probe liquids used are given in Table 4. Comparing these values (Figure 14), it can be seen that in particular it is the polar component that increases with aging time. The dispersive component remains constant over the time. The increase in the polar component of the surface free energy for sample BSP1 (with

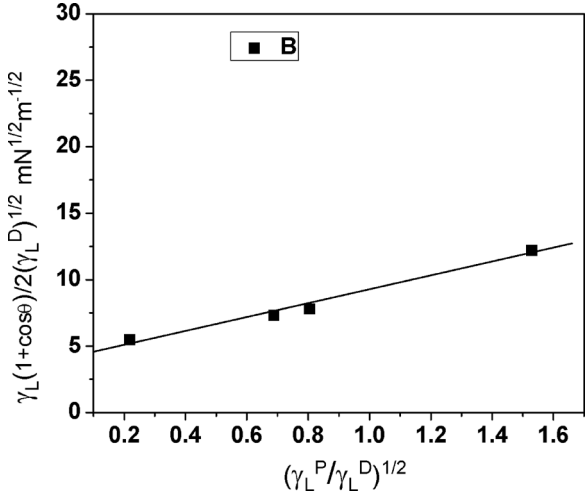

FIGURE 13 Plot based on Equation (9) for contact angle liquids against sample B.

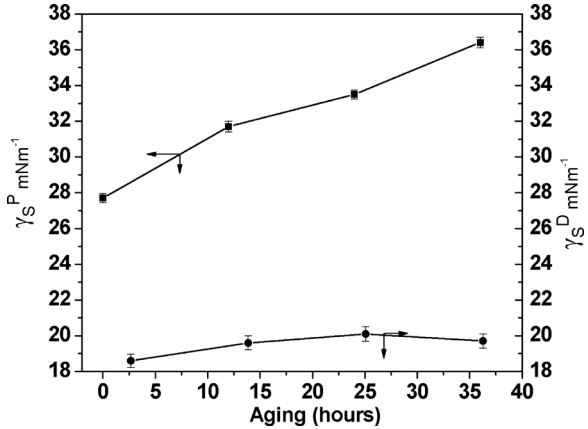

FIGURE 14 Experimental dispersive, γ_S^D, and polar, γ_S^P, component values of sample BSP1 (unaged and aged at 100°C at different time intervals).

aging time) clearly corresponds to the enrichment of the polar phenolic resin tackifier on the BIMS rubber surface upon aging.

FT-IR/ATR surface analyses of the samples B and BSP1 (unaged surface and aged surface) are shown in Figure 15. The FT-IR spectrum of phenolic resin is given as the inset of Figure 15. The peak assignments for phenolic resin are included in Table 5. BIMS shows peaks at 2995 cm^{-1}, 2853 cm^{-1}, and 813 cm^{-1} for asymmetric and symmetric C-H stretching of methyl and methylene groups and the 1,4-di-substituted benzene group, respectively. The peaks in the region of 450 cm^{-1} and 454 cm^{-1} are attributed to C-Br in BIMS rubber [35] (shown as inset of Figure 15). The FT-IR spectrum of the sample BSP1 (aged for 36 h) clearly shows a broad band in the region at 3400cm^{-1} (highlighted portion of the Figure 15), which is indicative of phenolic hydroxyl in the phenolic resin tackifier. However, this broad band region of phenolic hydroxyl groups was not identified in the case of the unaged BSP1 sample. This further corroborates the enrichment

TABLE 4 Literature Data on Contact Angle Probe Liquids

Sample number	Liquids	γ_L^D (m Nm^{-1})	γ_L^P (mNm^{-1})	Ref.
1	Water	21.8	51.0	32
2	Ethylene glycol	29.3	19.0	33
3	Formamide	39.5	18.7	33
4	Methylene diiodide	48.5	2.3	34

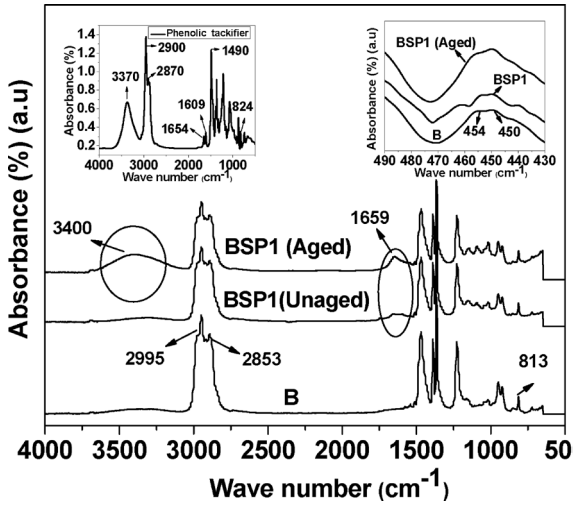

FIGURE 15 FT-IR spectra of sample B and BSP1 (unaged and aged at 100°C for 36 h). (Inset) FT-IR spectra of SP1068-phenolic resin tackifier.

of the phenolic resin tackifier on the BIMS rubber surface after aging. Furthermore, in the case of sample BSP1 (aged and unaged), one small new peak is identified in the region of 1659 cm^{-1}, which corresponds to aromatic modes of the phenolic resin in the rubber-resin mixture. Aging of the sample BSP1 resulted in an increase in the intensity of aromatic modes at 1659 cm^{-1} (highlighted portion of the Figure 15). This also confirms the increase in resin concentration in the surface region upon aging. Addition of phenolic resin to BIMS rubber changed the intensity of C-Br peaks of BIMS rubber (given as inset of Figure 15).

TABLE 5 FT-IR Peak Assignments for Phenolic Resin

Sample number	Frequency (cm^{-1})	Vibration
1	3360	Hydrogen bonded non-hindered phenol
2	2850 to 3000	CH stretching, suggest aliphatic groups with much methyl
3	1654, 1609, and 1490	Aromatic ring modes
4	Pair of bands at 1394 and 1364	$-C(CH_3)_3$
5	Pair of bands at 1385 and 1364	$-C(CH_3)_2$
6	1243	Aromatic C–O stretching
7	824	Suggest *p*-substitution

This is perhaps due to some chemical interaction between the phenolic hydroxyl group and C-Br group of the BIMS rubber.

4. CONCLUSIONS

The influence of a phenolic resin tackifier on the autohesion of uncrosslinked BIMS rubber was studied. Phenolic resin marginally increased the tack strength of the BIMS rubber at 1 phr resin loading. At higher resin loading, greater than 1 phr, there was a significant drop in the tack strength. The BIMS/phenolic resin blends containing tackifier concentration greater than 1 phr showed excess phase separation (blooming) of the tackifier on the rubber surface due the poor compatibility between the blend components. This reduced the true area of contact between the two joining surfaces and also seriously impaired the compression creep behavior and the viscoelastic properties of the rubber/resin mixtures required for good tack. After aging at 100°C for 36 h, the tack strength of the neat BIMS rubber was drastically reduced. Neat BIMS rubber was excessively softened and weakened due to aging. On the other hand, the tack strength of rubber/resin mixture containing 1 phr resin concentration showed further increment in tack strength upon aging at 100°C for 36 h. The further increase in the tack strength of the resin loaded sample upon aging was attributed to migration of the tackifier to the rubber surface and the changes in the compression creep, viscoelastic behavior, and maximum tensile stress of the rubber/resin mixtures. The preferential enrichment of the surface with polar phenolic resin upon aging significantly changed the surface composition and surface energy by modifying the surface polarity.

ACKNOWLEDGMENT

The authors are thankful to The ExxonMobil Chemical Co, USA, and ExxonMobil Chemical India Pvt. Ltd. for sponsoring the project and according permission to publish the results.

REFERENCES

[1] Voyutskii, S. S., *Autohesion and Adhesion of High Polymers*, (Interscience Publishers, New York, 1963), Ch. 1 and 2, pp. 5–59.
[2] Rhee, C. K. and Andries, J. C., *Rubber Chem. Technol.* **54**, 101–114 (1981).
[3] Hamed, G. R., *Rubber Chem. Technol.* **54**, 576–595 (1981).
[4] Skewis, J. D., *Rubber Chem. Technol.* **38**, 689–699 (1965).
[5] Wool, R. P., *Rubber Chem. Technol.* **57**, 307–319 (1984).
[6] Anand, J. N. and Karam, H. J., *J. Adhesion.* **1**, 16–23 (1969).

[7] Anand, J. N. and Balwinsky, R. Z., *J. Adhesion.* **1**, 24–30 (1969).
[8] Anand, J. N., *J. Adhesion.* **5**, 265–267 (1973).
[9] Roland, C. M. and Bohm, G. G. A., *Macromolecules* **8**, 1310–1314 (1985).
[10] Bhowmick, A. K. and Gent, A. N., *Rubber Chem. Technol.* **57**, 216–226 (1984).
[11] Bhowmick, A. K., De, P. P., and Bhattacharyya, A. K., *Polymer. Eng. Sci.* **27**, 1195–1202 (1987).
[12] Bhaumick, T. K., Gupta, B. R., and Bhowmick, A. K., *J. Adhesion Sci. Technol.* **1**, 227–238 (1987).
[13] Bhaumick, T. K., Gupta, B. R., and Bhowmick, A. K., *J. Adhesion.* **24**, 183–198 (1987).
[14] van Gunst, C. A., Paulen, H. J. G., and Wolters, E., *Kautschuk Gummi Kunststoffe.* **12**, 714–720 (1975).
[15] Hamed, G. R. and Magnus, F. L., *Rubber Chem. Technol.* **64**, 65–73 (1991).
[16] Powers, P. G., *Rubber Chem. Technol.* **36**, 1542–1570 (1991).
[17] Aubrey, D. W., *Rubber Chem. Technol.* **61**, 448–469 (1988).
[18] Sheriff, M., Knibbs, R. W., and Langley, P. G., *J. Appl. Polym. Sci.* **17**, 3423–3438 (1973).
[19] Dahlquist, C. A., *Kautschuk gummi Kunststoffe.* **38**, 617–620 (1985).
[20] Kumar, B., De, P. P., De, S. K., Peiffer, D. G., and Bhowmick, A. K., *J. Adhesion Sci. Technol.* **15**, 1145–1163 (2001).
[21] Duddey, J. E., Resins, in *Rubber Compounding: Chemistry and Applications*, M. B. Rodgers (Ed.) (Marcel Dekker, New York, 2004), Ch. 9, pp. 417–456.
[22] Class, J. B. and Chu, S. G., *J. Appl. Polym. Sci.* **30**, 805–814 (1985).
[23] Burhans, A. S. and Soldators, A. C., *Rubber Age.* **92**, 745–748 (1963).
[24] Fujita, M., Takemura, A., Ono, H., Kajiyama, M., Hayashi, S., and Mizumachi, H., *J. Appl. Polym. Sci.* **75**, 1535–1545 (2000).
[25] Tobing, S. D. and Klein, A., *J. Appl. Polym. Sci.* **76**, 1965–1976 (2000).
[26] Yuan, B., McGlinchey, C., and Pearce, E. M., *J. Appl. Polym. Sci.* **99**, 2408–2413 (2006).
[27] Ferry, J. D., *Viscoelastic Properties of Polymers*, (Wiley, New York, 1982), 3rd ed., Ch. 13, pp. 366–403.
[28] Counsell, P. J. C. and Whitehouse, R. S., *Developments in Adhesives*, W. C. Wake (Ed.) (Applied Science Publishers, London, 1977), Vol. I, Ch. 4, 99–126.
[29] Wetzel, F. H. and Alexander, B. B., *Adhesive Age.* **7**, 28–35 (1964).
[30] Paralusz, C. M., *J. Coll. Interf. Sci.* **47**, 719–746 (1974).
[31] Whitehouse, R. S. and Counsell, P. J. C., *Polymer* **17**, 699–704 (1976).
[32] Comyn, J., *Int. J. Adhesion and Adhesives* **15**, 9–14 (1995).
[33] Konar, J., Kole, S., Avasthi, B. N., and Bhowmick, A. K., *J. Appl. Polym. Sci.* **61**, 501–506 (1996).
[34] Comyn, J., Blackley, D. C., and Harding, L. M., *Int. J. Adhesion and Adhesives.* **13**, 163–171 (1993).
[35] Kumar, B., De, P. P., De, S. K., Peiffer, D. G., and Bhowmick, A. K., *J. Appl. Polym. Sci.* **82**, 1483–1494 (2001).